JOURNAL OF GEOPHYSICAL RESEARCH, VOL. 104, NO. D1, PAGES 1827–1836, JANUARY 20, 1999

Widespread solid particle formation by mountain waves in the Arctic stratosphere

Kenneth S. Carslaw and Thomas Peter
Max Planck Institute for Chemistry, Mainz, Germany

Julio T. Bacmeister[1]
Naval Research Laboratory, Washington, D.C.

Stephen D. Eckermann
Computational Physics, Inc., Fairfax, Virginia

Abstract. Observations of polar stratospheric clouds (PSCs) by lidar show that the clouds often contain solid particles, which are most likely composed of nitric acid hydrates. However, laboratory experiments indicate that such hydrate particles are not easily formed under Arctic synoptic scale conditions, suggesting that solid PSC particles should be rather rare. Here we show results from a model study indicating that mountain-induced mesoscale temperature perturbations may be an important source of nitric acid hydrate particles in the Arctic. Multiple Arctic vortex trajectories were combined with a global mountain wave forecast model to calculate the potential for solid particle formation during December and January 1994/1995. The mountain wave model was used to calculate adiabatic cooling over several thousand ridge elements. Nitric acid hydrate particles were assumed to form in the mountain waves according to several microphysical mechanisms, and were then advected using polar vortex-filling synoptic trajectories to generate maps of solid particle occurrence. The calculations show that mountain waves may be a significant source of PSCs containing solid particles that are observed on the synoptic scale. In particular, the east coast of Greenland, the Norwegian mountains, and the Urals are found to be solid particle sources, with the PSCs often predicted to survive several thousand kilometers downstream.

1. Introduction

Polar stratospheric clouds (PSCs) are frequently observed at temperatures above the ice frost point in the Arctic and are composed largely of condensed HNO_3 in various forms. Formation of liquid type 1 PSCs due to HNO_3 uptake by sulfuric acid-water aerosols to form large HNO_3-H_2SO_4-H_2O droplets is now well established [*Carslaw et al.*, 1994; *Drdla et al.*, 1994; *Tabazadeh et al.*, 1994; *Carslaw et al.*, 1997a; *Del Negro et al.*, 1997]. However, the mechanisms by which solid nitric acid-containing particles form are still unclear [e.g., *Peter*, 1997].

Lidar observations provide a means of distinguishing PSCs containing mostly liquid particles from those containing solid particles [*Browell et al.*, 1990; *Toon et al.*, 1990]. Although there exists no comprehensive climatology of solid and liquid PSC observations by lidar, the many data sets that have been reported in the literature indicate that solid particles are present in a large proportion of PSCs [*Browell et al.*, 1990; *Beyerle et al.*, 1994; *Stebel et al.*, 1997; *Nagai et al.*, 1997; *Biele et al.*, 1998; *Müller et al.*, 1998; *Neuber et al.*, 1998].

The phase of PSC particles has two potentially important effects on stratospheric chemistry. First, the rates of heterogeneous chlorine activation reactions are known to differ on liquids and solid nitric acid hydrates [*Ravishankara and Hanson*, 1996]. However, recent modeling studies suggest that these differences in reactivity may have a relatively minor effect on the overall rate of chlorine activation and subsequent ozone depletion over the course of an Arctic winter [*Carslaw et al.*, 1997b; *Becker et al.*, 1998]. Of more importance may be the potential of solid nitric acid-containing particles to denitrify the polar winter stratospheres. Denitrification, that is, the removal of odd-nitrogen species from the stratosphere (principally HNO_3), promotes the

[1]Now at the Universities Space Research Association, Columbia, Maryland.

Paper number1998JD100033.
0148-0227/99/1998JD100033$09.00

Report Documentation Page

Form Approved
OMB No. 0704-0188

1. REPORT DATE	2. REPORT TYPE	3. DATES COVERED
JAN 1999		**00-00-1999 to 00-00-1999**

4. TITLE AND SUBTITLE	5a. CONTRACT NUMBER
Widespread solid particle formation by mountain waves in the Arctic stratosphere	5b. GRANT NUMBER
	5c. PROGRAM ELEMENT NUMBER
6. AUTHOR(S)	5d. PROJECT NUMBER
	5e. TASK NUMBER
	5f. WORK UNIT NUMBER
7. PERFORMING ORGANIZATION NAME(S) AND ADDRESS(ES) **Naval Research Laboratory,Washington,DC,20375**	8. PERFORMING ORGANIZATION REPORT NUMBER
9. SPONSORING/MONITORING AGENCY NAME(S) AND ADDRESS(ES)	10. SPONSOR/MONITOR'S ACRONYM(S)
	11. SPONSOR/MONITOR'S REPORT NUMBER(S)

12. DISTRIBUTION/AVAILABILITY STATEMENT
Approved for public release; distribution unlimited

13. SUPPLEMENTARY NOTES

14. ABSTRACT
see report

15. SUBJECT TERMS

16. SECURITY CLASSIFICATION OF:			17. LIMITATION OF ABSTRACT	18. NUMBER OF PAGES	19a. NAME OF RESPONSIBLE PERSON
a. REPORT **unclassified**	b. ABSTRACT **unclassified**	c. THIS PAGE **unclassified**	**Same as Report (SAR)**	**10**	

halogen-catalyzed destruction of ozone. This depletion in HNO_3 is a characteristic feature of the Antarctic during winter but has also been observed in the Arctic [*Arnold et al.*, 1989; *Hübler et al.*, 1990; *Sugita et al.*, 1998]. The most likely cause of denitrification is gravitational settling of both ice particles (incorporating nitric acid) and large nitric acid hydrate (NAH) particles. Selective nucleation of a small number of NAH particles from an aerosol ensemble allows these particles to grow to sizes at which they have significant fall velocities, thus enabling them to remove nitric acid by sedimenting out of the polar stratosphere. The role of selectively nucleated NAH particles in denitrification remains to be confirmed, but it is likely to be the dominant process in the Arctic where temperatures are usually too high to support prolonged ice existence. The importance of solid nitric acid-containing particles in this respect makes their microphysical properties more than of academic interest.

Koop et al. [1997] have reviewed the processes leading to phase transformations in PSCs. Several mechanisms were identified that could account for the existence of solid particles in Arctic PSCs. These are summarized in the following five scenarios.

1.1. Scenario 1

Nitric acid hydrates could nucleate heterogeneously on water ice crystals below the ice frost point, leading to the release of NAH particles upon subsequent ice evaporation (shown as scenario 1 in Figure 1). Nitric acid hydrate formation by this mechanism can in principle operate on the synoptic scale, provided synoptic temperatures are low enough for the initial formation of ice. This is a strong constraint in view of recent work which suggests that liquid stratospheric aerosols can be supercooled by as much as 3 K below the ice frost point [*Koop et al.*, 1998] or even 4 K [*Carslaw et al.*, 1998a]. This would imply temperatures as low as 184-185 K on the 50 mbar pressure level in order to initiate the ice formation required for NAH particle nucleation. Ice-mediated NAH particle formation may be the dominant source of solid type 1 NAH-containing PSCs in the cold Antarctic stratosphere where ice PSCs occur frequently. However, large-scale ice occurrence is much less common in the Arctic stratosphere due to the higher temperatures, so an ice particle mediated NAH formation mechanism operating on the synoptic scale is unlikely to explain the large number of observations of PSCs containing solid particles in the Arctic. Indeed, many Arctic observations provide an indication for solid type 1 PSCs in air parcels that have remained above the ice frost point on the synoptic scale for several days [*Larsen et al.*, 1997]. However, as we show in this paper, mesoscale cooling events caused by mountain-induced gravity waves could increase the likelihood of NAH formation due to ice clouds.

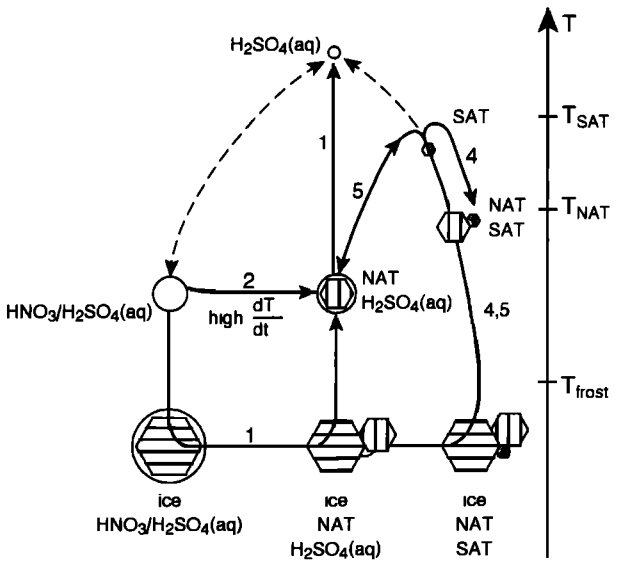

Figure 1. Particle phase transitions leading to the formation of solid type 1 PSC particles (NAT). The numbers 1-5 refer to the scenarios described in section 1. Note that the temperature axis is not to scale. A diagram showing many more particle phase transitions, from which this figure was taken, is given by *Koop et al.* [1997].

1.2. Scenario 2

Nitric acid hydrate particle nucleation might occur in non-equilibrium HNO_3-H_2SO_4-H_2O droplets in mountain waves, without ice formation (see Figure 1). This mechanism has been shown to operate in principle, based on model simulations and laboratory data [*Tsias et al.*, 1997], but there is as yet no observational evidence to confirm that solid PSC particles are generated in the stratosphere by this mechanism. A reliable simulation of NAH particle formation on the global scale via this mechanism is difficult since the heating and cooling rates required [*Tsias et al.*, 1997] are extreme and therefore not easily parameterized for global application.

1.3. Scenario 3

Tabazadeh et al. [1995] and *Tabazadeh and Toon* [1996] suggested that nucleation of solid HNO_3/H_2O phases might occur in air parcels that have spent sufficiently long below the nitric acid trihydrate (NAT) equilibrium temperature. They analyzed total aerosol volumes in a restricted aerosol size band as measured on board the ER-2 aircraft, and by assuming the particles were in thermodynamic equilibrium showed that the observations were inconsistent with NAT. They therefore postulated the existence of a new phase with a higher H_2O to HNO_3 ratio than either NAT or HNO_3-H_2SO_4-H_2O droplets, so called type 1c PSCs. An analysis of the measured particle size distributions underlying the integrated particle volumes [*Peter*, 1997] suggests an alternative explanation in terms of well established solid phases. Nevertheless, as already stated, the origin of these solids remains unclear.

1.4. Scenario 4

Zhang et al. [1996] have suggested that nitric acid hydrates may form on frozen sulfuric acid aerosols (sulfuric acid tetrahydrate (SAT)) after their surfaces have become activated by an initial deposition of NAT (see Figure 1). The supersaturation required for NAT nucleation on preactivated SAT particles corresponds to about a 2-3 K cooling below the NAT equilibrium temperature. Such a preactivation mechanism was shown to operate efficiently in the laboratory and may indeed operate in the stratosphere.

1.5. Scenario 5

Koop and Carslaw [1996] have shown that SAT particles can deliquesce to form HNO_3-H_2SO_4-H_2O droplets upon cooling to temperatures a few K above the ice frost point (typically 3-4 K below the NAT equilibrium temperature, see Figure 1). They suggested that this mechanism might lead to the heterogeneous nucleation of NAT. Recent laboratory experiments by *Iraci et al.* [1998] appear to confirm the heterogeneous nucleation of NAT on deliquescing SAT. However, a similar study [*Martin et al.*, 1998] indicates that the deliquescence of SAT may not occur readily in the stratosphere. This NAT formation mechanism, if effective, would compete with the preactivation mechanism of *Zhang et al.* [1996]. The extent to which NAH particles are produced by either mechanism 4 or 5 depends on the how many of the background aerosols are present as SAT. There is presently little evidence for SAT particles in the stratosphere, which is unlikely to form by homogeneous nucleation of liquid aerosols, but rather via heterogeneous nucleation on either NAT or ice [*Koop et al.*, 1997]. Hence, NAT formation via the *Zhang et al.* [1996] or *Koop and Carslaw* [1996] mechanisms may occur in air parcels that have already supported ice PSC formation. We return to this possibility later.

All of these mechanisms have conceptual difficulties if they are to account for the presence of solid particles in type 1 PSCs in the Arctic [*Peter*, 1997]. The direct formation of NAH PSCs from liquid HNO_3-H_2SO_4-H_2O aerosols was discounted by *Koop et al.* [1997] on the basis of laboratory experiments. Scenario 1 requires temperatures to fall below the ice frost point, which occurs rarely on the synoptic scale; scenario 2 has yet to be confirmed by field observations; scenario 3 relies on the difficult comparison of observed aerosol volumes and equilibrium models to confirm a new solid PSC type; scenarios 4 and 5 rely upon the existence of SAT particles, which at best form only after ice PSCs have already existed.

In this work we consider the possibility that solid PSC particles are formed via mechanism 1 in mountain-induced gravity waves rather than on the synoptic scale. The recent work of *Carslaw et al.* [1998a] supports this possibility. Their analysis of aircraft lidar observations reveals that ice clouds that formed in mountain waves over Norway acted as a source of solid-containing type 1 PSCs that persisted downwind of the mountains. Furthermore, *Carslaw et al.* [1998b] have calculated that for the winter 1994/95, temperatures may have passed below the ice frost point in mountain waves as often as once every 17 days in air parcels confined within the Arctic vortex. They showed that as much as half of the vortex air could be processed below the ice frost point by December 20, 1994, while synoptic temperatures never fell this low. This rate of occurrence of mountain waves with temperatures below the frost point suggests that they might act as a significant source of localized ice clouds and hence solid nitric acid hydrate particles.

Tabazadeh et al. [1996] have examined aircraft lidar data for possible influences of mesoscale activity. They concluded that only about half of the PSCs containing solid particles could be attributed to mountain wave cooling events. However, they restricted their analysis to a single day and to a relatively small region of the northern hemisphere. Here we consider the potential impact of mountain waves for a 2 month period over the entire Arctic vortex. We also show that if scenarios 4 or 5 operate, then NAT formation may occur in air parcels even several weeks after an initial wave encounter, thus making an analysis based on a limited number of back trajectories very difficult.

2. Method of Calculation

We calculate the frequency with which mountain waves are encountered by air parcels confined within the Arctic polar vortex. The flow of air parcels was calculated using 500 vortex-filling trajectories on three different potential temperature levels. By coupling this information with several realistic NAH particle formation mechanisms we assess the potential for mountain waves to generate solid PSC particles.

2.1. Mountain Wave Activity

Calculation of mountain wave cooling over such a large geographical area and for a whole winter first requires a reliable parameterization of stratospheric mountain wave activity. We use the orographic gravity wave parameterization of *Bacmeister et al.* [1994]. This is based on a global database of dominant topographic "ridge" features, which contains estimates of ridge height, width, and orientation. Synoptic analyses of wind and temperature at standard pressure levels between the ground and 10 mbar are then used to determine air flow over these ridge features, and subsequent generation of mountain waves. Here we use the National Center for Environmental Prediction (NCEP) analyses at $5° \times 2°$ resolution. A two-dimensional (2-D) hydrostatic gravity wave model is used in conjunction with the NCEP winds and temperatures to simulate the subsequent amplification, dissipation, and/or critical-level filtering of these waves as they propagate away from the ridge to higher regions of the atmosphere.

Advection of air by hydrostatic gravity waves is isentropic to a good approximation, so that air parcel tem-

peratures vary in response to wave-induced vertical advection according to the dry adiabatic lapse rate [*Eckermann et al.*, 1998]. At any instant, this yields a (reversible) temperature perturbation ΔT from the background temperature. In the present study, it is the adiabatic cooling ($\Delta T < 0$) that is of primary significance, since reversible episodes of wave-induced cooling have major effects on PSC microphysics and chemistry. We neglect the adiabatic warming phase in the mountain waves ($\Delta T > 0$) as a loss mechanism of nucleated NAH particles. This warming is often of short enough duration in mountain waves that NAH particles do not completely evaporate before temperatures fall again [*Tsias et al.*, 1997; *Carslaw et al.*, 1998a].

The intrinsic frequency of the wave ω determines the adiabatic heating/cooling rate perturbation, $\partial T/\partial t$, within the parcel. However, we do not use this information to simulate scenario 2 since the high heating/cooling rates required for solid particle formation in gravity waves [*Tsias et al.*, 1997] are likely to occur under non hydrostatic conditions and cannot therefore be described by this simplified model.

The maximum wave-induced adiabatic cooling $\Delta T_{\max}$ (i.e., maximum negative departure of the air parcel temperature from that expected on the synoptic scale) was calculated for each ridge element that generated a mountain wave which reached the stratosphere on a given day. These values $\Delta T_{\max}(x_0, z)$ were derived from the wave amplitudes in the mountain wave model, which provides a vertical profile (z = altitude) centered directly above the central ridge position x_0. A horizontal "influence function" was then applied to simulate the likely horizontal spread of mountain wave activity some distance away from the ridge center. Here we used

$$\Delta T(x, z) = \Delta T_{\max}(x_0, z) \exp\left[-(x - x_0)^2/w^2\right] \quad (1)$$

to simulate cooling downsteam of the ridge ($x > x_0$), and

$$\Delta T(x, z) = \Delta T_{\max}(x_0, z) \exp\left[-10(x - x_0)^2/w^2\right] \quad (2)$$

for cooling values upstream of the ridge ($x < x_0$), where x is the downstream distance from the "ridge line" in the orthogonal or "cross-ridge" direction, and w is the cross-ridge width. This Gaussian influence function represents a simplified but plausible wave amplitude envelope above a 2D ridge, with more energy found downstream of the ridge than upstream, as suggested by case studies. The temperature change is assumed to be zero in extension of the ridge axis.

2.2. Vortex-Filling Trajectories

The technique of using multiple trajectories that fill a region of the atmosphere (domain filling) provides an ideal means of assessing PSC formation by small ridge elements. We have used 500 isentropic 60-day trajectories on the 400, 475, and 550 K potential temperature surfaces, chosen to be confined within the Arctic polar vortex between December 1, 1994 and January 31, 1995. Trajectories were calculated from NCEP analyses with a 1 hour time step. The air parcels remained evenly distributed within the vortex during this period, thus providing a reliable statistical view of the flow over mountain waves on a given potential temperature surface. This technique correctly describes the rate of airflow through individual mountain waves on a given potential temperature level as well as correctly describing the lifetime of solid particles in air parcels that undergo synoptic cooling and heating cycles as they circle the pole.

We have used isentropic trajectories so that the PSC formation resulting from mountain waves can be conveniently identified with a given potential temperature surface. Clearly, the air flow is actually diabatic during the 2 month period being considered, with the air sinking perhaps as much as 4 or 5 km between December 1 and January 31. However, the assumption of isentropic flow need only be valid for the short time that nitric acid hydrate particles exist in an air parcel, which, due to periodic warming over the Alaskan sector of the polar vortex, is typically less than 2-3 days in the Arctic. The 60-day trajectories can therefore be considered equivalent to a sequence of many shorter quasi-isentropic trajectories. We have also compared the results obtained with these isentropic trajectories with similar calculations that take account of diabatic motion. The results confirmed the validity of assuming short-term quasi-isentropic flow.

The mountain wave database was searched for coincidences at every 1-hour trajectory step and for every trajectory. A coincidence occurs where a straight line connecting the current and previous trajectory locations cuts the influence region of one or more waves. Where two or more waves overlapped, the greater of the two peak temperature changes ($\Delta T_{\max}$) was taken. The peak temperature change was linearly interpolated between pressure levels to obtain $\Delta T_{\max}$ for the pressure level of the trajectory. The minimum air parcel temperature between two trajectory points was determined along a straight line cutting the mountain wave influence region. The formation of nitric acid trihydrate (NAT) by various mechanisms was then examined at this minimum temperature. We have made similar calculations with as few as 100 trajectories, with very similar results. This suggests that the chosen 500 trajectories provide a good statistical representation of solid particle formation in mesoscale cooling events.

2.3. Formation of Solid PSC Particles

The formation of NAT particles in the mountain waves was investigated based on scenarios 1, 4, and 5. Ice and NAT equilibrium temperatures were calculated according to *Hanson and Mauersberger* [1988] assuming a water vapor mixing ratio that varied with altitude as

follows: 400 K (4.2 ppmv); 475 K (4.6 ppmv); 550 K (5.4 ppmv). In the absence of a representative HNO_3 altitude profile a constant 10 ppbv HNO_3 on all levels was used.

According to scenario 1, ice was assumed to nucleate in liquid droplets 4 K below the ice frost point ($T_{frost} - 4$ K) allowing NAT to form heterogeneously. The remaining small amount of H_2SO_4 and H_2O in each frozen particle was assumed to remain liquid, leading to the release of NAT particles internally mixed with H_2SO_4/H_2O upon ice evaporation. Such particles would be composed principally of NAT and would appear in lidar observations as solid particles due to their depolarization of the return signal. Upon further warming above the NAT equilibrium temperature, pure liquid droplets are released, thus resetting the particle phase to the initial conditions.

Note that we do not say anything about the number density of NAT particles in a given air parcel, but only whether the air parcel contains such particles or not. In fact, number densities of NAT particles exiting mountain waves are known to be quite low [*Carslaw et al.*, 1998a]. We also do not say anything about the size of the individual NAT particles, which may often be far from thermodynamic equilibrium with HNO_3 in the gas phase [*Peter*, 1997; *Tsias et al.*, 1997; *Carslaw et al.*, 1998a]. The effect of slow growth and evaporation kinetics probably acts to increase the geographical area containing solid particles, which is not taken into account in the present simulation.

The amount of supercooling with respect to ice before crystalization is an important parameter in the model since this represents a barrier to ice and NAT formation in the waves, thus reducing the amount of NAT that can be released onto the synoptic scale. For example, for typical conditions on the 50 mbar level, temperatures must fall as low as 183 K before ice formation, which is a considerable cooling below typical synoptic temperatures in the Arctic winter stratosphere. Our assumption of 4 K supercooling is in agreement with the analysis of mountain wave PSCs performed by *Carslaw et al.* [1998a] but larger than the approximate 2 K suggested by the theoretical work of *Tabazadeh et al.* [1997] and the earlier experiments on H_2SO_4/H_2O droplets [*Bertram et al.*, 1996]. More recent laboratory experiments examining the freezing of H_2SO_4/H_2O droplets suggest that ice forms approximately 3 K below the ice frost point under typical stratospheric conditions [*Koop et al.*, 1998], a somewhat greater supercooling than suggested by *Bertram et al.* [1996]. We therefore consider our assumed 4 K supercooling to be an upper limit to the supercooling requirement. In the sensitivity calculations we explore the effect of changing this quantity.

According to scenarios 4 and 5, SAT particles can serve as sites for NAT nucleation at temperatures a few K above the ice frost point. To simulate these mechanisms, we assume that ice formation in the mountain waves leads to complete crystallization of the remaining liquid HNO_3-H_2SO_4-H_2O to form NAT and SAT (see Figure 1). Subsequent warming then releases NAT/SAT mixed particles above T_{frost} and pure SAT particles above T_{NAT}. These SAT particles can then support NAT formation according to either scenario 4 or 5. Scenario 4 was simulated by allowing NAT to form at a supersaturation of 10 (approximately 3 K below T_{NAT}). In scenario 5, NAT forms upon cooling below the SAT deliquescence point, which is typically 3-4 K below T_{NAT} (the SAT deliquescence temperature was calculated in terms of the HNO_3 and H_2O partial pressures using the thermodynamic model of *Carslaw et al.* [1995]). The effect of these mechanisms is to amplify the NAT production due to mountain waves alone; SAT particles that are released from mountain waves and suffer a further cooling cycle can serve as sites for NAT nucleation at several degrees higher temperature than would otherwise be required if only mechanism 1 operated. These "additional" NAT particles may form either on the synoptic scale when temperatures fall sufficiently low or in mountain waves that are too warm to support ice nucleation.

Air parcels containing NAT particles were advected downstream by the domain-filling trajectories and were assumed to persist in the air parcel until temperatures rose above T_{NAT}, at which point NAT was assumed to evaporate immediately. Some mountain waves are sufficiently vigorous that ice and NAT particles may form in the wave although synoptic temperatures are higher than the NAT equilibrium temperature. No production of persistent synoptic scale NAT occurs in such cases, although these waves may still contribute to chlorine activation in the air parcel [*Carslaw et al.*, 1998b].

3. Mountain PSC Formation and NAT Production

3.1. Scenario 1

Plate 1 shows maps of NAT occurrence (black streaks) for December 1994 and January 1995 together with locations where temperatures fell below $T_{frost} - 4$K (red dots). Figure 2a shows a time series of the number of model air parcels containing NAT particles as a fraction of the 500 trajectories on the 475 K level. The distribution of ice-forming mountain waves (Plate 1), and hence NAT production, is strongly biased toward the European and Siberian sector of the northern hemisphere, where low synoptic temperatures coincide with strong wave activity. Although strong mountain wave cooling occurs over Alaska, synoptic temperatures in this part of the polar vortex (Aleutian high) are persistently warmer than over the European sector, which prevents ice formation in these waves.

Gravity wave amplitudes often increase with increasing altitude due to the reduction in air density, hence the number of very cold waves ($T < T_{frost} - 4$ K) and their geographical spread increases with increasing al-

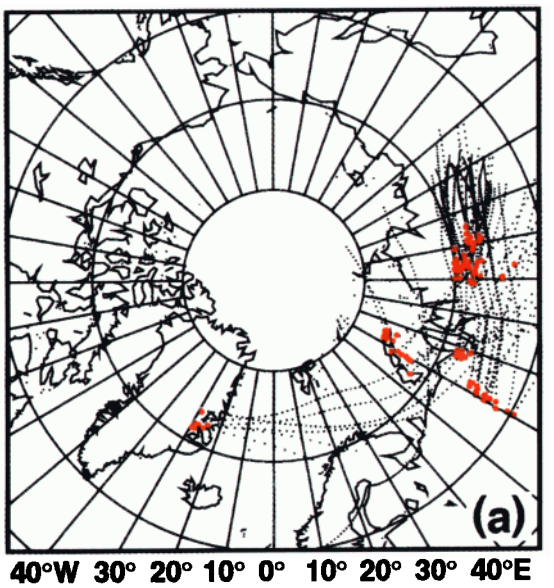

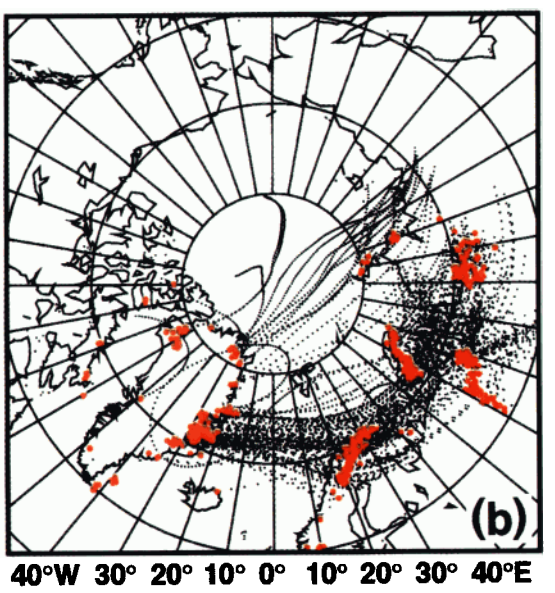

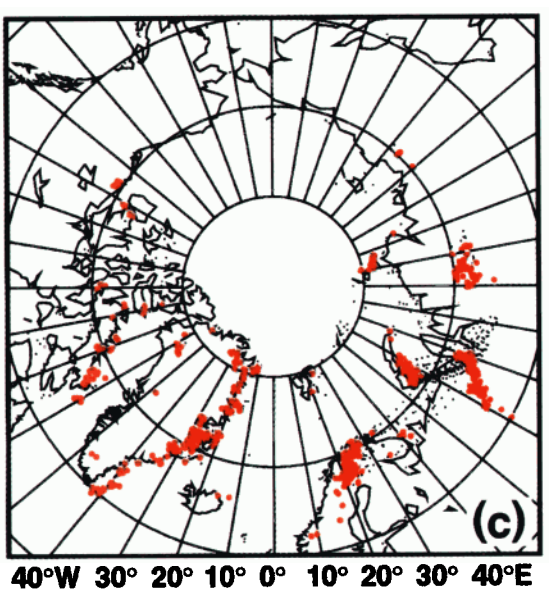

titude (potential temperature). On the 400 K level (~16 km altitude), most of these events occur over the Siberian mountains at 90°–100°E with a few on the east coast of Greenland. On the 475 K level (~19 km) the mountains of East Greenland, Scandinavia, the Urals, and Novaya Zemlya are all apparent, while on the 550 K level (~22 km) strong mountain waves are apparent even over Baffin Island (60° – 70°W) and farther west.

The Scandinavian mountains act as a significant source of NAT particles that extend over Scandinavia, particularly on the 475 K level. The east coast of Greenland also generates NAT particles that survive the passage over the North Atlantic, where temperatures are often below T_{NAT} over a wide area. PSCs containing solid particles observed over Scandinavia may therefore often originate several thousand kilometers upstream. NAT particles generated over the Siberian mountains (90°E) generally persist only a few hours before evaporating in the warmer temperatures that are persistent over the Alaskan sector of the polar vortex. Although the wave amplitudes and number of very cold waves are greatest on the 550 K level, the number of model air parcels containing NAT is very small, reflecting the generally higher synoptic temperatures on that level relative to the NAT equilibrium temperature. The fewer number of air parcels containing NAT on the 400 and 550 K levels is also due to the location of the polar vortex relative to significant orography. On the 475 K level the area where temperatures below T_{NAT} occur covered most of the region between 60°W – 150°E and north of 65°N. In contrast, the potential NAT area on the 550 K level was restricted to $\simeq$ 20°W (the East Greenland coast), 110°E and north of $\simeq$ 68°N. Hence, on the 550 K level, NAT particle persistence downwind of the East Greenland coastal mountains and the northern Scandinavian mountains was severely restricted.

The number of air parcels containing NAT (Figure 2a) fluctuates in response to the extent of low temperatures in the vortex. During cold periods, both the production rate of NAT in the mountain waves and the lifetime of the generated NAT particles are greater. The

Plate 1. Geographical distribution of mountain wave-induced NAT PSCs during December 1994 and January 1995 on the levels (a) 400 K, (b) 475 K, and (c) 550 K according to scenario 1. Air parcels calculated to contain NAT particles are marked with a black dot at each trajectory step (1 hour intervals). NAT particles were assumed to be produced in air parcels where the temperature passed below $T_{frost} - 4$ K (red dots) leading to ice formation. Note that the red dots are placed at the nearest trajectory point location and therefore may be displaced away from the ridge element that induced the adiabatic cooling event. Synoptic temperatures during the 2 month period were such that no NAT formation was assumed to occur other than in mountain waves. The calculation refers to 500 trajectories.

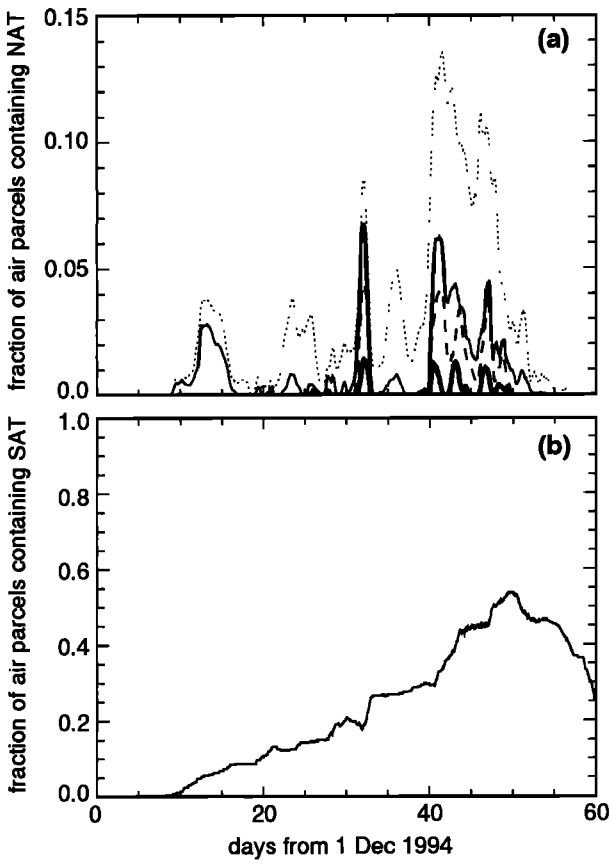

Figure 2. (a) Fraction of the 500 model air parcels containing NAT particles, plotted at 1 hour intervals. Thin solid line, assuming ice forms at $T_{\text{frost}} - 4$ K (scenario 1, corresponding to the map in Plate 1); dotted line, assuming NAT forms upon SAT deliquescence (scenario 5); thick solid line, a sensitivity test using scenario 1 in which all wave amplitudes were reduced by a factor of 2; dashed line, a sensitivity test using scenario 1 but with all wave amplitudes reduced by a factor of 2 and synoptic temperatures reduced by 2 K overall. (b) Fraction of air parcels containing SAT particles according to scenario 5.

fraction of model air parcels containing NAT (induced through the action of mountain waves) is as much as 5% on the 475 K level, equivalent to a total area of 6×10^5 km^2 if these air parcels are considered representative of 5% of the vortex air. Much lower coverages are predicted for the 400 and 550 K levels. If NAT were allowed to form whenever temperatures fell below the NAT equilibrium temperature, then the maximum areal coverage of NAT in the vortex would be about 20%. This implies that NAT is present in approximately 25% of the vortex area where NAT is stable. Locally, the areal coverage of NAT can be much higher. For example, downwind of the Scandinavian mountains more than 50% of the model air parcels are calculated to contain NAT particles on January 11, 1995 (day 42 in Figure 2).

3.2. Scenarios 4 and 5

The effect of NAT production through SAT deliquescence (scenario 5) leads to a considerable increase in the area of the vortex containing NAT (dotted line in Figure 2a); about a factor of 2 increase compared with scenario 1 in mid-January, and sometimes as much as a factor of 6 increase. NAT is predicted to fill up to 14% of the vortex on the 475 K level, or about 2×10^7 km^2.

It is interesting to note that the amount of air containing SAT particles increases steadily during December and early January (Figure 2b). Temperatures during this period generally remain below the SAT melting temperature of 210-215 K, thus SAT generated in mountain waves accumulates in the vortex (note that NAT formation upon SAT deliquescence does not lead to the loss of SAT particles since these are assumed to be recovered once the NAT evaporates again). By mid-January as much as 50% of the vortex is calculated to contain some SAT. The amount of SAT falls only in late January as temperatures increase and the loss rate of SAT by melting exceeds the production rate in mountain waves. Note that the assumption of isentropic air parcel behavior is not strictly valid for the much longer times (up to several weeks) that SAT particles exist in a given air parcel. To test the results in Figure 2b, we have performed similar calculations based on diabatic trajectories cutting the 475 K level (as used by *Carslaw et al.* [1998b]) and obtained very similar results to those shown here.

Particularly important in terms of being able to attribute NAT formation in the stratosphere to a particular mechanism is that in many of the air parcels NAT formation upon SAT deliquescence occurred several weeks after the initial mountain wave event. Attributing a given solid-particle PSC observation to mountain waves might therefore prove very difficult if this SAT-deliquescence mechanism operates. Such NAT PSCs may also be more uniform in structure than those derived directly from mountain waves due to the atmospheric mixing that occurs during the few weeks.

An alternative to the SAT deliquescence mechanism is the preactivation mechanism of *Zhang et al.* [1996] (scenario 4). In their mechanism, NAT can form on SAT at a supersaturation with respect to NAT, S_{NAT}, of $\sim$10. This corresponds to a temperature of about 2-3 K below the NAT equilibrium temperature, T_{NAT}, under normal stratospheric conditions. Formation of NAT by this process is therefore likely to occur more often than by the SAT deliquescence mechanism, which requires that temperatures fall about 4 K below T_{NAT}. Whether NAT formation due to SAT preactivation or SAT deliquescence operates in the stratosphere is not certain. A sensitivity test in which NAT formed via the preactivation mechanism led to calculated NAT amounts generally about 30% higher than predicted by assuming NAT formation upon SAT deliquescence (20% NAT coverage of the vortex compared with 15%).

3.3. Sensitivity Tests

There are several factors that may change the production of solid particles initiated by mountain waves. We

show how these might affect the foregoing calculations for the 475 K level also in Figure 2a.

3.3.1. Reduction in wave amplitudes. We have considered the effect of reducing the magnitude of adiabatic cooling in all waves (thick solid line in Figure 2a). *Bacmeister et al.* [1994] and later *Carslaw et al.* [1998a] have compared the predictions of the Bacmeister et al. model with observations of mountain wave cooling. They found reasonable agreement between predicted and observed adiabatic temperature excursions for large-amplitude waves where ΔT was 10-20 K. However, there is some indication that the model somewhat overestimates the wave amplitude for less vigorous waves. A comparison with waves observed by the ER-2 over the southern tip of Greenland suggests that the Bacmeister et al. model overestimated the wave amplitude by about 50% ($\Delta T \simeq 12$ K compared with an observed 8 K). As a sensitivity test, we have reduced all wave amplitudes by a factor of 2. This leads to a considerable reduction in the amount of mountain wave-initiated NAT. NAT is predicted to occur on only a few days in January and to be present in less than ~1.5% of the vortex, or 1.5×10^5 km^2. The maximum spatial extent of SAT particles in the vortex reaches about 6% of the vortex area, hence even allowing for NAT production through SAT deliquescence does not significantly increase the amount of NAT.

3.3.2. Bias in synoptic temperatures. The dashed line in Figure 2a shows the results of a simulation with all mountain wave amplitudes reduced by a factor of 2, as above, but with the synoptic temperatures decreased by 2 K overall. This leads to NAT coverage in the vortex as much as a factor of 3-4 greater than predicted by reducing the wave amplitudes alone and reveals the enormous sensitivity of NAT production to temperature, which arises due to the combined increase in the number of ice PSCs occurring in the waves as well as the extended persistence of NAT on the synoptic scale.

3.3.3. Ice supercooling requirement. A further test was made by reducing the amount of supercooling required for ice formation in the waves from 4 K to 2 K (results not shown). Changing the supercooling requirement for ice formation affects only the efficiency of NAT production but not the persistence of NAT on the synoptic scale. The fraction of model air parcels containing NAT was therefore between that predicted for the sensitivity tests described in 3.3.1 and 3.3.2. Increasing the amount of water vapor on the 475 K level to 5 ppmv changes the ice frost point and NAT equilibrium temperatures by less than 0.5 K and therefore does not significantly affect these results.

4. Discussion

The model simulations presented above reveal that NAT production due to mountain waves depends very sensitively on a number of parameters. The most sensitive, in order of importance, are (1) the magnitude of adiabatic cooling in each wave, (2) the synoptic temperature, and (3) the supercooling required for initial ice formation. The model simulations suggest that some mountain wave-induced solid particles are likely to be present in the polar vortex when temperatures are low enough to support nitric acid hydrates, but the current uncertainties in model parameters do not allow the calculated areal coverages to be well constrained (coverages of NAT are calculated to lie between 1 and 14% of the vortex area on the 475 K level, or, equivalently, between about 4 and 60% of the vortex area where temperatures are below the NAT equilibrium temperature). Directly downwind of the Scandinavian mountains, more than 50% of the air on a single level may contain mountain wave-induced NAT under favorable conditions. Our calculations did not take account of mixing of NAT-containing air parcels into the surrounding air. This would serve to increase the fraction of the polar vortex containing some NAT particles.

The magnitude of the adiabatic cooling is a particularly uncertain parameter. Our test calculations assumed that the adiabatic cooling predicted by the Bacmeister et al. model might be too large by up to a factor of 2. This is equivalent to a reduction in the cooling in large waves from $\Delta T \simeq 20$K to $\Delta T \simeq 10$K, a far greater uncertainty than in the supercooling required for initial ice formation ($\Delta T \simeq 4$K). The effect of this reduction in model wave amplitudes was to reduce the areal coverage of NAT by more than a factor of 3, or even to switch off NAT production completely. Adiabatic cooling in mountain waves by as much as $\Delta T \simeq 12 - 19$K has been inferred from observations of ice clouds over Norway [*Carslaw et al.*, 1998a,b], suggesting that a uniform reduction in predicted wave amplitudes may be unrealistic. Further work is clearly required to validate the mountain wave forecast model that we have used. However, it is worth pointing out that a realistic reduction in model wave amplitudes, which would result by introducing dispersion of wave energy in the horizontal, will lead to a much wider influence region around each ridge element in the model. This in turn will result in more vortex air being processed through mountain waves, which might partly compensate for the reduced peak cooling.

There is clear evidence for the formation of ice in mountain waves and the subsequent release of solid particles downwind of the mountains [*Carslaw et al.*, 1998a]. However, the crystallization of the remaining H_2SO_4 to form sulfuric acid hydrates such as SAT is less certain. While SAT formation in mountain waves is not a requirement for solid particle formation, we showed that subsequent deliquescence of SAT upon cooling (followed by NAT formation [*Koop and Carslaw*, 1996]) or nucleation of NAT on preactivated SAT particles [*Zhang et al.*, 1996] could act as an efficient additional NAT source.

We have also highlighted that the fraction of the polar vortex containing mountain wave-generated NAT par-

ticles depends on the location of low temperatures relative to the Greenlandic and Scandinavian mountains. In particular, the east coast of Greenland can serve as a source of solid PSC particles that flow over Europe provided that temperatures are below T_{NAT} over the North Atlantic. Interannual changes in the location of the vortex and associated low temperatures could therefore strongly influence the amount of mountain wave-generated solid-containing PSCs.

A related factor is that the largest amplitude gravity waves are sustained in the stratosphere under conditions where the stratospheric winds are strongest. The location of the polar-night jet (or polar vortex edge) relative to the region of lowest stratospheric synoptic tempertures is therefore also important. Particularly important for the effectiveness of mountain waves in generating NAT is that the coldest region of the polar vortex can sometimes lie close to or on the vortex edge. Under these conditions, the potential for sustaining large wave amplitudes (highest stratospheric winds) combines with the maximum likelihood that NAT will presist on the synoptic scale (lowest synoptic temperatures). Considerable NAT production due to mountain waves might therefore be expected during these periods.

Direct comparison between observations of solid-containing PSCs and the predicted location of NAT clouds originating from mountain waves should be made with caution. The mountain wave climatology used here should predict the general location and magnitude of wave activity on a statistical basis. However, individual back trajectories constructed for comparison with PSC observations cannot be expected to yield reliable statistical information on NAT production. We have also shown that NAT formation as a result of SAT deliquescence close to the frost point [*Koop and Carslaw*, 1996; *Iraci et al.*, 1998] could disguise any direct link between observed solid particles and the initiating mountain wave.

Larsen et al. [1997] have performed the most complete statistical analysis of the synoptic conditions under which PSCs are likely to be observed in the solid or liquid phase. Their investigation, based on 30 balloonsonde flights over 4 years from seven ground stations in the Arctic, reveals that the likelihood of solid and liquid PSCs depends very much on the synoptic conditions prior to the observation. In particular, the occurrence of PSCs containing solid particles was shown to be more likely in air parcels that had spent a considerable time below the NAT equilibrium temperature, while liquid aerosols occur most frequently in air parcels that have cooled recently. Our proposed mechanism, in terms of mountain wave NAT activation, is qualitatively consistent with these statistics; the more time air spends at low temperatures the greater is the probability that a mountain wave will force the temperature low enough to induce ice formation and hence solidification of the HNO_3-H_2SO_4-H_2O solutions. The likelihood of NAT activation upon SAT deliquescence is also greater at lower temperatures since the deliquescence temperature is about 3-5 K below the NAT equilibrium temperature.

Future work should extend the study presented here to include a quantitative comparison with PSC observations. Such a study should aim to establish, as far as possible, the number of solid particle-containing PSC observations that can be explained by mountain wave processes. One approach would be to compile a lidar climatology, with PSCs being classified according to a threshold value of depolarization.

Acknowledgments. Funded partly by the European Community under contract ENV4-CT95-0050 and the German BMBF under contract 01 LO 9506/0.

References

Arnold, F., H. Schlager, J. Hoffmann, P. Metzinger, and S. Spreng, Evidence for stratospheric nitric acid condensation from balloon and rocket measurements in the Arctic, *Nature, 342*, 493-497, 1989.

Bacmeister, J.T., P.A. Newman, B.L. Gary, and K.R. Chan, An alogorithm for forecasting mountain wave-related turbulence in the stratosphere, *Weather and Forecasting, 9*, 241, 1994.

Becker, G., R. Müller, D.S. McKenna, M. Rex, and K.S. Carslaw, Ozone loss rates in the Arctic stratosphere in the winter 1991/92: Model caculations compared with Match results, *Geophys. Res. Lett.*, in press, 1998.

Bertram, A.K., D.D. Paterson, and J.J. Sloan, Mechanisms and temperatures for the freezing of sulfuric acid aerosols measured by FTIR extinction spectroscopy, *J. Phys. Chem., 100*, 2376-2383, 1996.

Beyerle, G., R. Neuber, O. Schrems, F. Wittrock, and B. Knudsen, Multiwavelength lidar measurements of stratospheric aerosols above Spitsbergen during winter 1992/93, *Geophys. Res. Lett., 21*, 57-60, 1994.

Biele, J., et al., The evolution of polar stratospheric clouds above Spitsbergen in winter 1996/97, in *Polar Stratospheric Ozone 1997, Proceedings of the 4th European Symposium, 22 to 26 September 1997, Schliersee, Bavaria, Germany*, edited by N.R.P. Harris, I. Kilbane-Dawe, and G.T. Amanatidis, European Communities, Luxembourg, 1998.

Browell, E.V., C.F. Butler, S. Ismail, P.A. Robinette, A.F. Carter, N.S. Higdon, O.B. Toon, M.R. Schoeberl and A.F. Tuck, Airborne lidar observations in the wintertime Arctic stratosphere: Polar stratospheric clouds, *Geophys. Res. Lett., 17*, 385-388, 1990.

Carslaw, K.S., B.P. Luo, S.L. Clegg, Th. Peter, P. Brimblecombe, and P. Crutzen, Stratospheric aerosol growth and HNO_3 gas phase depletion from coupled HNO_3 and water uptake by liquid particles, *Geophys. Res. Lett., 21*, 2479-2482, 1994.

Carslaw, K.S., S.L. Clegg and P. Brimblecombe, A thermodynamic model of the system HCl-HNO_3-H_2SO_4-H_2O including solubilities of HBr, from <200 K to 328 K, *J. Phys. Chem., 99*, 11557-11574, 1995.

Carslaw, K.S., Th. Peter, and S.L. Clegg, Modeling the composition of liquid stratospheric aerosols, *Rev. Geophys., 35*, 125-154, 1997a.

Carslaw, K.S., Th. Peter, and R. Müller, Uncertainties in reactive uptake coefficients for solid stratospheric particles,II, Effect on ozone depletion, *Geophys. Res. Lett., 24*, 1747-1750, 1997b.

Carslaw, K.S., et al., Particle microphysics and chemistry in

remotely observed mountain polar stratospheric clouds, *J. Geophys. Res., 103*, 5785-5796, 1998a.

Carslaw, K.S., et al., Increased stratospheric ozone depletion due to mountain-induced atmospheric waves, *Nature, 391*, 675-678, 1998b.

Del Negro, L.A., et al., Evaluating the role of NAT, NAD, and liquid HNO_3-H_2SO_4-H_2O solutions in Antarctic polar stratospheric cloud aerosol: Observations and implications, *J. Geophys. Res., 102*, 13255-13282, 1997.

Drdla, K., A. Tabazadeh, R.P. Turco, M.Z. Jacobson, J.E. Dye, C. Twohy, D. Baumgardner, K.K. Kelly, R.P. Chan and M. Loewenstein, Analysis of the physical state of one Arctic polar stratospheric cloud based of observations, *Geophys. Res. Lett., 21*, 2473-2478, 1994.

Eckermann, S. D., D. E. Gibson-Wilde, and J. T. Bacmeister, Gravity wave perturbations of minor constituents: A parcel advection methodology, *J. Atmos. Sci.*, in press, 1998.

Hanson, D., and K. Mauersberger, Laboratory studies of the nitric acid trihydrate: Implications for the south polar stratosphere, *Geophys. Res. Lett., 15*, 855-858, 1988.

Hübler, G., et al., Redistribution of odd nitrogen in the lower Arctic stratosphere, *Geophys. Res. Lett., 17*, 453-456, 1990.

Iraci, L.T., T.J. Fortin, and M.A. Tolbert, Dissolution of sulfuric acid tetrahydrate at low temperatures and subsequent growth of nitric acid trihydrate, *J. Geophys. Res., 103*, 8491-8498, 1998.

Koop, T., and K.S. Carslaw, Melting of $H_2SO_4 \cdot 4H_2O$ particles upon cooling: Implications for polar stratospheric clouds, *Science, 272*, 1638-1641, 1996.

Koop, T, K.S. Carslaw, and Th. Peter, Thermodynamic stability and phase transitions of PSC particles, *Geophys. Res. Lett., 24*, 2199-2202, 1997.

Koop, T. H.P. Ng, L.T. Molina, and M.J. Molina, A new optical technique to study aerosol phase transitions: The nucleation of ice from H_2SO_4 aerosols, *J. Phys. Chem.*, in press, 1998.

Larsen, N., B.M. Knudsen, J.M. Rosen, N.T. Kjome, R. Neuber, and E. Kyrö, Temperature histories in liquid and solid polar stratospheric cloud formation, *J. Geophys. Res., 102*, 23505-23517, 1997.

Martin, S.T., D. Salcedo, L.T. Molina, and M.J. Molina, Deliquescence of sulfuric acid tetrahydrate following volcanic eruptions or denitrification, *Geophys. Res. Lett., 25*, 31-34, 1998.

Müller, K.P., G. Baumgarten, J. Siebert, and K.H. Fricke, PSC observations with the new lidar facility at Esrange, Kiruna in winter 1996/97, in *Polar Stratospheric Ozone 1997, Proceedings of the 4th European Symposium, 22 to 26 September 1997, Schliersee, Bavaria, Germany*, edited by N.R.P. Harris, I. Kilbane-Dawe, and G.T. Amanatidis, European Communities, Luxembourg, 1998.

Nagai, T., O. Uchino, T. Itabe, T. Shibata, K. Mizutani, T. Fujimoto, and M. Hirota, Lidar observations of the PSCs and stratospheric aerosols over Eureka in Canadian Arctic, in *Advances in Atmospheric Remote Sensing with Lidar, Selected Papers of the 18th International Laser Radar Conference (ILRC), Berlin, 22-26 July, 1996*, edited by A. Ansmann et al., Springer-Verlag, New York, 1997.

Neuber, R., P. von der Gaathen, J. Biele, J. Rosen, and H. Gernandt, The effect of different PSC particles on local ozone depletion during the Arctic winter 96/97, in *Polar Stratospheric Ozone 1997, Proceedings of the 4th European Symposium, 22 to 26 September 1997, Schliersee, Bavaria, Germany*, edited by N.R.P. Harris, I. Kilbane-Dawe, and G.T. Amanatidis, European Communities, Luxembourg, 1998.

Peter, Th., Microphysics and chemistry of polar stratospheric cloud particles, *Annu. Rev. Phys. Chem., 48*, 785-822, 1997.

Ravishankara, A.R., and D.R. Hanson, Differences in the reactivity of type I polar stratospheric clouds depending on their phase, *J. Geophys. Res., 101*, 3885-3890, 1996.

Stebel, K., R. Neuber, G. Beyerle, J. Biele, P. Scheuch, H. Schütt, P. von der Gaathen, and O. Schrems, Lidar observations of polar stratospheric clouds above Spitsbergen, in *Advances in Atmospheric Remote Sensing with Lidar, Selected Papers of the 18th International Laser Radar Conference (ILRC), Berlin, 22-26 July, 1996*, edited by A. Ansmann et al., Springer-Verlag, New York, 1997.

Sugita, T., et al., Denitrification observed inside the Arctic vortex in February 1995, *J. Geophys. Res., 103*, 16221-16233, 1998.

Tabazadeh, A., and O.B. Toon, The presence of metastable HNO_3/H_2O solid phases in the stratosphere inferred from ER 2 data, *J. Geophys. Res., 101*, 9071-9078, 1996.

Tabazadeh, A., R.P. Turco, K. Drdla, M.Z. Jacobson, and O.B. Toon, A study of type I polar stratospheric cloud formation, *Geophys. Res. Lett., 21*, 1619-1622, 1994.

Tabazadeh, A., O.B. Toon, and P. Hamill, Freezing behavior of stratospheric sulfate aerosols inferred from trajectory studies, *Geophys. Res. Lett., 22*, 1725-1728, 1995.

Tabazadeh, A., O.B. Toon, B.L. Gary, J.T. Bacmeister, and M.R. Schoeberl, Observational constraints on the formation of type Ia polar stratospheric clouds, *Geophys. Res. Lett., 23*, 2109-2112, 1996.

Tabazadeh, A., O.B. Toon, and E.J. Jensen, Formation and implications of ice particle nucleation in the stratosphere, *Geophys. Res. Lett., 24*, 2007-2010, 1997.

Toon, O.B., E.V. Browell, S. Kinne, and J. Jordan, An analysis of Lidar observations of polar stratospheric clouds, *Geophys. Res. Lett., 17*, 393-396, 1990.

Tsias, A., A. Prenni, K.S. Carslaw, T.P. Onasch, B.P. Luo, M.A. Tolbert, and T. Peter, Freezing of polar stratospheric clouds in orographically induced strong warming events, *Geophys. Res. Lett., 24*, 2303-2306, 1997.

Zhang, R., M.-T. Leu, and M.J. Molina, Formation of polar stratospheric clouds on preactivated background aerosols, *Geophys. Res. Lett., 23*, 1669-1672, 1996.

J. T. Bacmeister, Universities Space Research Association, 10227 Wincopin Circle, Suite 202, Columbia, MD 21044. (e-mail: bacmj@janus.gsfc.nasa.gov)

K. S. Carslaw and Th. Peter, Max-Planck-Institut für Chemie, Postfach 3060, Mainz 55020, Germany. (e-mail: carslaw@mpch-mainz.mpg.de; peter@mpch-mainz.mpg.de)

S. Eckermann, E. O. Hulbert Center for Space Research, Code 7641, Naval Research Laboratory, Washington, D.C. 20375. (e-mail: eckerman@ismap4.nrl.navy.mil)

(Received June 18, 1998; revised September 21, 1998; accepted September 24, 1998.)